Available online at www.sciencedirect.com
SCIENCE DIRECT
Journal of Catalysis 241 (2006) 56–65
JOURNAL OF CATALYSIS
www.elsevier.com/locate/jcat

Evaluation of the Au size effect: CO oxidation catalyzed by Au/TiO_2

S.H. Overbury [a,*], Viviane Schwartz [a], David R. Mullins [a], Wenfu Yan [a,b], Sheng Dai [a]

[a] *Oak Ridge National Laboratory, Oak Ridge, TN 37831-6201, USA*
[b] *State Key Laboratory of Inorganic Synthesis and Preparative Chemistry, College of Chemistry, Jilin University, Changchun 130012, China*

Received 8 February 2006; revised 11 April 2006; accepted 13 April 2006
Available online 30 May 2006

Abstract

The size dependence of activity in gold catalysts was examined. Extended X-ray absorption fine structure was used to determine mean particle size, and a flow reactor was used to assess activity of the catalysts for CO oxidation as a function of temperature. A sequence of calcination steps was used to systematically increase the mean Au particle size while repeated measurements of the activity were conducted. In this way the size dependence could be obtained in a single catalyst to avoid differences due to variations in support, synthesis conditions, Au loading, or incidental impurities. Two Au catalysts with different Au loadings were prepared on TiO_2 by deposition precipitation and used for the measurements. For Au particles with mean particle size, d, in the range of 2–10 nm, the measured TOF at 298 K varies as $d^{-1.7\pm0.2}$ and $d^{-0.9\pm0.2}$ for the 7.2 and 4.5 wt% Au/TiO_2 (P25) catalysts, respectively. Variation between samples emphasizes the conclusion that the activity is sensitive to many factors that may mask the true structure dependence. It is concluded that the observed decrease in activity with increasing particle size beyond 2 nm is controlled by the population of low-coordinate sites, rather than by size-dependent changes in overall electronic structure of the nanoparticle. No evidence was found for maximum activity for small particle sizes, although arguments are offered for why such a maximum was expected but was not observed.

Keywords: Structure sensitivity; Size sensitivity; Catalytic CO oxidation; Gold catalysts; Au; TiO_2; EXAFS; XANES; Flow reactor; Catalytic activity

1. Introduction

Size dependency in Au catalysis is widely accepted, much discussed, but still not clearly understood. Seminal work by Haruta et al. [1] demonstrated that the activity of supported Au catalysts for CO oxidation increases sharply with decreasing Au particle size below 4 nm, from which it was concluded that the reaction is "structure-sensitive." It was suggested that active sites for oxygen adsorption are those at the interfacial perimeter around the Au metal particles, and that this could be the source of the size sensitivity. Subsequent work concentrating on TiO_2 further demonstrated the size (structure) dependence [2]. In that study it was observed that preparation methods had a substantial effect on activity, again presumably due to variation in the perimeter interface as controlled by the preparation conditions. Throughout the past decade, there have been many studies of CO oxidation by Au catalysts, and the roles of many factors related to activity have been identified and explored. Researchers have correlated activity with support type in terms of "inert" versus "active" supports [3] or the reducibility of the support [4], with the effect of water [5,6], with residual Cl^- concentration [7], with Au loading [8], and with the effects of various deposition methods [9–11]. The sensitivity of Au catalysts to these and other experimental factors complicates the comparison of results from different laboratories and hinders an understanding of the relationship between size or structure and activity of Au particles.

Nonetheless, progress has been made. Using STM to determine the size of Au particles deposited on $TiO_2(110)$ in UHV, then measuring CO oxidation activity in an appendage reactor, Valden and Goodman demonstrated the size effect for a model system [12]. Subsequent work has suggested that high activity is associated with a particular structural site that is optimal for a two-layers-thick Au raft [13]. This interpretation is reminiscent of counting special multicoordinated sites (e.g., the B5 sites) postulated to explain "volcano"-size dependencies seen

* Corresponding author.
E-mail address: overburysh@ornl.gov (S.H. Overbury).

0021-9517/$ – see front matter
doi:10.1016/j.jcat.2006.04.018

in other catalysts and reactions [14,15]. Many theoretical models have been proposed to describe and explain the available experimental results [16,17]. Various geometric and physical parameters have been investigated, including changes in the periphery area, proportion of defect sites (edge, step, or kink sites on the surface of Au crystallites), support-induced strain, coordination of active Au atoms, and size-induced variation in the electronic properties of the Au. Such analysis relies on comparisons of results from several labs, which requires care in identifying and compensating for the effects of "uninteresting" experimental factors. Recently, size-selected Au clusters "soft-landed" on oxide films were used to probe quantum size effects on the properties of the Au clusters [18] and provided evidence that activity may turn off for Au clusters smaller than about 8 atoms.

To clarify the size effect, it is necessary to obtain careful measurements of the catalyst particle size distribution and correlate this closely with measured reaction rate under uniform reaction conditions. This should be done for a series of catalysts in which the particle size distribution is systematically varied without varying any other parameters that could affect the catalyst. Optimally, the size distribution should be obtained while the reaction is demonstrated to be proceeding or at least under reaction conditions. Despite the work described above, it can be argued that there are not sufficient experimental data in which all of the foregoing conditions are met. To date, most measurements of particle size versus activity for practical Au catalysts have been done by measurement of reaction rates, followed by measurement of the particle sizes by ex situ electron microscopy [1,2,9]. From the mean particle diameter, the surface area and hence the Au dispersion is estimated, usually assuming spherical particles. Such an approach is necessitated in part by difficulties in the direct measurement of Au surface area due to gas uptake. Uncertainty arises from the unknown effect of removing the sample from the reaction environment to perform microscopy, and care must be taken to assure that the size distribution of selected micrographs represents the catalyst as a whole. Another uncertainty may arise from the difficulty of detecting thin, raft-like Au particles by TEM [19]. Such small rafts may be present in large numbers on the Au catalysts and dominantly contribute to the reactivity, but be undercounted in TEM measurements of the mean particle size. On an active catalyst, Z-contrast microscopy is capable of detecting large quantities of raft-like Au particles on TiO_2 (anatase), which are generally not visible by TEM [19]. An alternative approach is to use extended X-ray absorption fine structure (EXAFS) analysis instead of TEM to obtain mean particle size. This approach may be more sensitive to small raft-like particles. EXAFS averages over the entire volume of catalyst and may possibly provide more accurate sampling of the overall mean particle size. In addition, EXAFS is more adaptable than TEM for determining mean particle size under reaction conditions. But even though EXAFS is expected to be favorable for very small particles, it is not suitable for particles larger than about 5–10 nm. In addition, it gives little information about distribution of sizes and has difficulty delineating particle shapes.

We have addressed these issues by measuring the activity for CO oxidation coupled with in situ EXAFS to obtain mean Au particle size. In what follows, we report measurements of the activity of two TiO_2-supported Au catalysts as a function of Au particle size. The Au particle size in each catalyst is varied by a sequence of annealing treatments that are found to systematically increase the size of the Au particles. Using this approach, a correlation between particle size and activity can be achieved for a single catalyst without complications due to variable synthesis conditions that would otherwise be necessary to systematically vary particle size. The results are interpreted in light of evidence on variation in reaction mechanisms and pitfalls of assessing catalytic activity for catalysts that depend sensitively on particle size.

2. Experimental

2.1. Sample preparation

Au catalysts were prepared on commercial Degussa P25 TiO_2 supports using deposition precipitation. Weighed amounts of hydrogen tetrachloroaurate (III) trihydrate ($HAuCl_4 \cdot 3H_2O$, 99.9+%, Aldrich) were dissolved into 50 mL of deionized water. The pH value of the resulting solution was adjusted to 9.0–10.0 with vigorous stirring, using a solution of 1.0 M KOH at room temperature to displace Cl^- with hydroxyl on the Au(III) precursor. After pH adjustment, the solution was heated in a 60 °C water bath, after which 1.0 g of TiO_2 powder was added. The resulting mixture was continually stirred for 2 h to permit the Au precursor to react with and displace surface hydroxyls. Finally, the precipitates were separated by centrifugation and washed three times with deionized water and once with ethanol to remove Cl^-. The product was dried at 50 °C in air overnight to obtain the "as-synthesized" catalyst. Two batches of Au catalysts were produced using amounts of $HAuCl_4$ to yield Au loadings of 13 and 6.5 wt% if all Au were to adsorb on the TiO_2. Catalysts were analyzed for Au and chloride impurities by ion-coupled plasma (ICP) technique, which determined actual Au loadings of 7.2 and 4.5 wt% and Cl^- levels of 313 and 349 ppm for the two samples. To prevent the growth of Au particles and other changes in the catalysts, no calcinations or reductions were performed on the catalysts until they were placed into the catalytic reactor for catalytic measurement or for EXAFS analysis.

2.2. X-Ray absorption spectroscopy measurements

The X-ray absorption spectroscopy (XAS) data at the Au L_{III}-edge were collected at beamline X18b at the NSLS, Brookhaven National Laboratory. A Si(111) crystal was used as a monochromator, and the crystal was detuned by 20% at the Au L_{III}-edge to reject higher harmonics. The XAS was performed in transmission mode using two ion chambers placed in the beam path. Absorption measurements were made in a quartz tube (50 cm long × 2.4 cm diameter) which could be heated for sample treatments or cooled for EXAFS measurements. For each run, a weighed amount of fresh catalyst (about

100 mg) was mixed with 100 mg of BN and loosely pressed into a 12-mm-diameter pellet. (BN was added to provide structural integrity to the wafer without interfering with X-ray absorption.) X-Ray absorption near-edge spectroscopy (XANES) was performed under reduction, calcination, or reaction conditions. EXAFS measurements were obtained under He after the reactor cell was cooled to about 135 K, to minimize thermal disorder, which can lead to high Debye–Waller factors.

The program XDAP, version 3.2 was used to analyze and fit the data [20]. In brief, the data reduction procedure involved the following steps: pre-edge subtraction, background determination, normalization, and spectra averaging. First, the pre-edge was approximated by a modified Victoreen curve and subtracted from the whole data range. The edge position is defined as the first inflection point on the leading absorption peak. This was calibrated to be 11,919 eV for the L_{III}-edge of an Au reference foil. The background in the EXAFS region was approximated using a cubic spline routine and optimized according to the criteria described by Cook and Sayers [21]. Then the spectra were normalized by the edge step at 50 eV after the absorption edge. The k^3-weighted and k^1-weighted EXAFS functions were Fourier-transformed, filtered, and fitted in R space. Fourier filtering was used to isolate the contributions of specific shells and to eliminate low-frequency background and high-frequency noise. Fourier filtering is done by choosing a window in the Fourier transform spectrum and calculating the inverse Fourier transform of the selected R range. The interatomic distance, r; the first nearest-neighbor coordination number, 1NN; the difference of the Debye–Waller factor from the reference, $\Delta\sigma^2$; and the correction of the threshold energy, ΔE^0, were treated as free parameters during the fitting. The quality of the fit was estimated from the values of k^3 variance, V_{k^3}. The variance represents the residual between the observed and calculated spectrum in the fitted range; low values of variance indicate a good agreement between data and model. Fitting analysis in both k^1- and k^3-weighted Fourier transforms was applied to obtain a unique set of 1NN and $\Delta\sigma^2$ parameters. These parameters are highly correlated, and a number of different combinations of 1NN and $\Delta\sigma^2$ can lead to similar fits; however, the set of combinations depends on the k weight factor. Therefore, a unique set of parameters might be found by fitting on both k^1- and k^3-weighted Fourier transforms. To analyze the spectra, simulations of reference compounds using FEFF8.1 [22] were used to calculate phase shifts and backscattering amplitude. FEFF references were obtained for Au–Au using crystallographic data of Au metal and by measuring Au foil.

2.3. Activity measurements

On-line activity measurements were carried out to assess catalyst activity during the XAS measurements. The quartz sample tube was set up to operate as a continuously recirculating stirred tank reactor in a way that did not interfere with XAS measurements. A mass spectrometer was used to sample the gas in the reactor. Because significant mass flow problems were suspected in the on-line activity measurements, the catalyst activities were also measured off-line (i.e., not at the synchrotron). These measurements were performed in a plug-flow reactor (Altamira AMI-200) with a gas chromatograph used to analyze the exit gas composition and quantify the CO conversion. Weighed amounts of the fine, as-synthesized catalysts (from the same batches as used for the EXAFS measurements) were mixed with 150–200 mg of inert quartz sand to better distribute the heat of reaction. The powder was supported on quartz wool plug on the rising side of a quartz U-tube with a 4-mm inside diameter, making a plug about 15 mm long. The reactant gas was a dry mixture of 1% CO in air (Air Liquide) that was used without further purification. The water content was specified by the manufacturer to be <5 ppm. Activity was measured at a flow/weight (F/W) ratio of 10,000–400,000 mL/(g_{cat} h). Initially, about 50 mg of catalyst was used with a flow rate of around 33 mL/min, but because the measured range of activity varied by orders of magnitude, additional measurements were also made for other sample weights and flows. To achieve lower conversions for the most active catalysts, measurements were performed using less catalyst (5 or 20 mg) and comparable flow rates, thereby increasing the F/W ratio up to an order of magnitude. For the least active catalysts, measurements were made at lower F/W, achieved by decreasing the reactant flow rate.

After each sample treatment, activity was measured as a function of temperature. During this phase, the sample temperature was allowed to increase very slowly (from as low as 0.1 K/min up to 0.5 K/min) to simulate quasisteady-state reactions. In some cases, repeated measurements were made at a fixed temperature (room temperature or 273 K) by monitoring the conversion under a steady flow rate over 1–2 h. A 1-mL portion of the product stream was extracted periodically with an automatic sampling valve for analysis by dual-column gas chromatography (GC) with a thermal conductivity detector. The incoming reactant stream was used to calibrate the GC response to CO, and the product stream from a catalyst under conditions of 100% conversion was used to calibrate the CO_2 peak intensity. Measured CO conversion was used along with gas flow rate and the mass and Au loading of the catalyst to calculate what we call the *atomic rate* in moles of CO converted per mole of *total* Au per second.

3. Results

3.1. EXAFS/XANES results

X-Ray absorption measurements were carried out on each sample following a sequence of thermal treatments intended to bring about a systematic increase in Au particle size. First, fresh catalyst was reduced at 425 K for 30 min in hydrogen and then cooled in the hydrogen to near room temperature. At this point, the reaction mixture was introduced, and CO conversion was measured at one or more temperatures near room temperature. The cell was then purged with He and cooled for measurement of the EXAFS spectrum. Subsequently, the sample was calcined at elevated temperature, and the sequence of cooling, activity measurement, and EXAFS was repeated. Calcination was performed at increasing temperatures, each followed by activity and low-temperature EXAFS measurements. One set

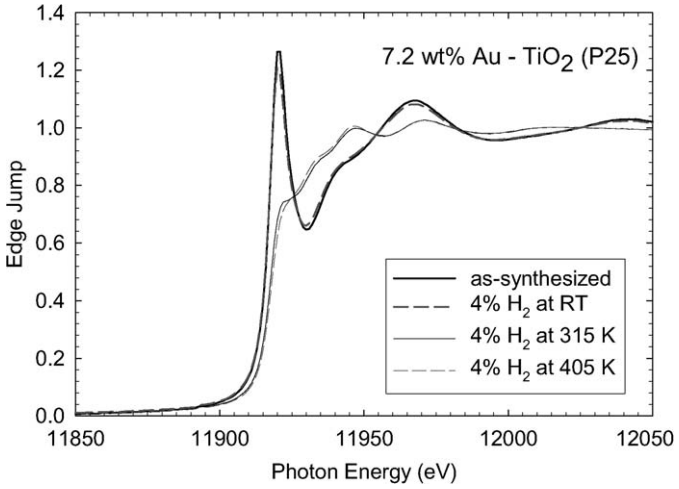

Fig. 1. Au L_{III} XANES spectrum obtained while increasing the temperature of the 7.2 wt% Au/TiO_2 (P25) sample under flowing 4% H_2–He.

of samples was calcined at 573, 673, and 773 K, holding for 20 or 30 min at each temperature. A second set was calcined at 573, 623, 673, 723, and 773 K, holding at 20 min at each temperature.

The XANES results indicate that Au was readily reduced by the initial treatment in flowing hydrogen at 425 K. Fig. 1 shows a typical set of XANES recorded during the ramp up to 425 K in hydrogen. As described previously for other TiO_2-supported Au catalysts [8], the sample was significantly reduced by this treatment. Reduction was indicated by the loss of the pre-edge peak, which occurred already by about 375 K for the 4.5 wt% sample and by 315 K for the 7.2 wt% sample. Measurements were also made following the calcination steps, and it was found that subsequent treatments in air did not lead to reoxidation of the Au, consistent with previous reports [8].

Fig. 2 shows typical EXAFS results obtained after a set of thermal treatments for the 7.2 wt% Au/TiO_2 (P25) sample. Analysis of the EXAFS data were carried out to obtain the properties of the first coordination shell of the Au atoms; the results for both runs of the two samples are given in Tables 1 and 2. Values of the parameters used in the fit are also included. Inspection of the data in Fig. 2 clearly indicates that the sequential thermal treatments caused a steady increase in intensity in the peak corresponding to the first Au shell, a result expected with increasing Au particle size. The coordination numbers extracted from analysis of the data help quantify the particle growth, and, as seen in Tables 1 and 2, they increased steadily with increasing treatment temperature, approaching the bulk value of 12 after calcination at 775 K. In addition, a corresponding increase in the Au–Au nearest-neighbor distance (from 2.83 to 2.87 Å) and a decrease in the mean squared relative displacement (from 65 to 35 $\times$ 10^{-4} $Å^2$) are apparent in the fitted results. These trends are also associated with the growth of particles and have been reported previously [8,23–25].

3.2. Activity measurements

Activity of the catalysts was measured in the XAS cell immediately after each treatment and before cooling in He for

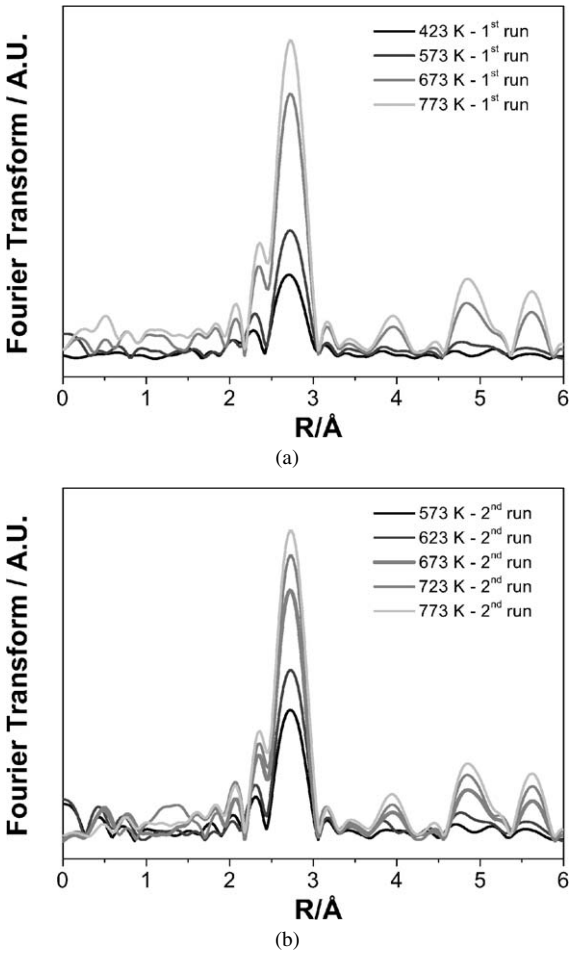

Fig. 2. Fourier transform of the EXAFS spectra are shown for the 7.2 wt% Au/TiO_2 (P25) sample following sequential reduction (at 425 K) and calcination at increasing temperatures. Results from the first run (a) and the second run (b) are shown. Transforms are obtained from the k^3-weighted data for a k range of about 3.45 to 18.

measurement of the EXAFS. These on-line measurements were valuable for demonstrating that the samples were active for CO oxidation near room temperature after the treatments. However, the measured conversion did not change strongly with reaction temperature or with heat treatment, contrary to the results under the off-line conditions. Thus, it was concluded that the on-line measurements did not accurately represent the true activity of the catalyst, possibly due to mass transfer limitations associated with the flow patterns in the cell or the pellet form of the catalysts required by the EXAFS measurements. Therefore, to better characterize how the activity depends on the thermal treatments, the catalytic activity of the catalysts was also measured in an off-line reactor. In these off-line measurements, the fine, nonporous catalyst powder resulting from the synthesis was used directly without pelletization or sieving, and there was no indication of the type of mass transfer limitations observed in the on-line measurements.

A sequence of treatments at increasing temperatures was used in the off-line measurements; these mimic the treatments performed during the synchrotron measurements. As such, the catalyst was first reduced in H_2 to 423 K, and the same sample

Table 1
EXAFS results for 7.2 wt% Au/TiO_2 (P25), analysis of the first Au–Au shell

Treatment temperature (K)	Run	1NN	R (Å)	$\Delta\sigma^2 \times 10^{-4}$ (Å^2)	ΔE^0 (eV)	$V^3_{k\text{-fit}}$	d[a] (nm)
423	1st	8.4	2.83	66	−3.7	0.73	2.0
	2nd	n/a	n/a	n/a	n/a	n/a	
573	1st	8.7	2.85	53	−4.7	0.72	2.0
	2nd	7.9	2.85	48	−4.9	0.66	
623	1st	b	b	b	b	b	3.0
	2nd	9.5	2.85	46	−4.2	0.52	
673	1st	10.2	2.86	37	−4.6	0.64	4.5
	2nd	9.9	2.86	36	−4.4	0.11	
723	1st	b	b	b	b	b	6.5
	2nd	10.6	2.87	35	−5.0	0.56	
773	1st	11.1	2.87	33	−4.4	0.25	10.2
	2nd	11.4	2.87	34	−4.5	0.45	

The errors in the final parameters are expected to be: CN ± 10%; $R \pm 0.02$ Å; $\Delta\sigma^2 \pm 20\%$; and $\Delta E^0 \pm 20\%$. The 1st run was performed using soaking time of 30 min, 2nd run using soaking time of 20 min. n/a – Annealing step completed but EXAFS was not run.

[a] Particle diameter (average of both runs) obtained from the 1NN coordination number and based upon a truncated cubo-octahedron model [25].

[b] Denotes that annealing step omitted for this sample.

Table 2
EXAFS results for 4.5 wt% Au/TiO_2 (P25); analysis of the first Au–Au shell

Treatment temperature (K)	Run	1NN	R (Å)	$\Delta\sigma^2 \times 10^{-4}$ (Å^2)	ΔE^0 (eV)	$V^3_{k\text{-fit}}$	d[a] (nm)
423	1st	8.7	2.84	62	−3.3	1.66	1.8
	2nd	7.2	2.83	65	−4.8	0.51	
573	1st	8.0	2.85	54	−5.0	1.91	2.1
	2nd	8.9	2.85	61	−4.4	1.38	
623	1st	b	b	b	b	b	2.6
	2nd	9.1	2.85	46	−4.6	0.35	
673	1st	10.8	2.86	43	−4.7	1.01	5.0
	2nd	9.8	2.86	39	−4.2	0.33	
723	1st	b	b	b	b	b	6.0
	2nd	10.5	2.86	35	−4.9	0.59	
773	1st	11.4	2.87	35	−4.8	0.45	11.8
	2nd	12	2.87	37	−4.6	0.73	

The errors in the final parameters are expected to be: CN ± 10%; $R \pm 0.02$ Å; $\Delta\sigma^2 \pm 20\%$; and $\Delta E^0 \pm 20\%$. Both runs used soaking time of 20 min.

[a] Particle diameter (average of both runs) obtained from the 1NN and based upon a truncated cubo-octahedron model [25].

[b] Denotes that annealing step omitted for this sample.

was then calcined at a sequence of increasingly higher temperatures. The activity was measured after each calcination step. The crucial assumption is that reproducing the heat treatment conditions performed on-line during the X-ray absorption measurements would reproduce the sintering of the Au particles. All activity measurements provided below are from the off-line measurements. Data are presented as a function of temperature and for various F/W ratios [26].

Fig. 3 shows typical results, plotted as a function of temperature in an Arrhenius form for a single F/W condition. To approximate differential conditions, only CO conversions below about 40% should be considered. The detection limit of the

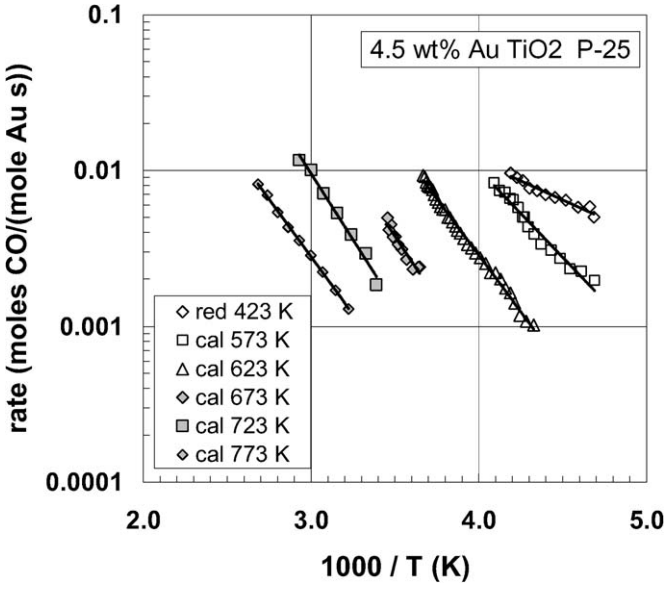

Fig. 3. Reaction rate of the 4.5 wt% Au/TiO_2 (P25) catalyst measured for 49 mg catalyst and $F/W = 40{,}000$ mL CO/(g_{cat} h). Rate is expressed per total amount of Au in the catalyst (atomic rate). The catalyst was heated for 30 min at each of the indicated temperatures, in order of increasing temperature. After each temperature, the sample was cooled and the activity vs. temperature curve was measured. Fitted lines used for extrapolation of the rates are shown.

CO_2 peak requires conversion in excess of a few percent. Based on the above limits of conversion, for a fixed F/W of 40,000, only atomic rates between 0.001 and 0.01 are accessible. As the catalyst activity changes due to thermal treatments, different temperature ranges must be sampled to determine the reaction rates. This explains the offset temperature ranges shown in Fig. 3. The figure indicates that the rate at any given temperature generally decreases as the temperature of calcination increases, suggesting thermally induced deactivation of the Au catalyst.

To compare activity at a single temperature (e.g., 298 or 273 K), some of the data must be extrapolated. The assumption of Arrhenius behavior permits this extrapolation, but may be invalid if the reaction mechanism, and thus the activation energy, depends on temperature. Measurements were also made using other F/W values, which allows differential conditions to be maintained over various temperature ranges. Fig. 4 shows typical results for the 7.2 wt% Au/TiO_2 (P25) catalyst obtained for other values of F/W. Table 3 summarizes all data obtained from both samples. For each catalyst, the rates were measured in two or more runs; for example, for the 4.5 wt% Au sample, two runs were made, each with the same weight of catalyst, both of which are included in Table 3. The data indicate differences between the extrapolated rates and the activation energies obtained by linear regression. The atomic rates of the most active catalysts are in the range of $1–3 \times 10^{-2}$ mol CO/(mol total Au s) at 273 K, in good agreement with several previous measurements [3,9,16,27–29].

4. Discussion

Comparing the data given in Figs. 3 and 4 at a given temperature shows variation in the atomic rate by more than two or-

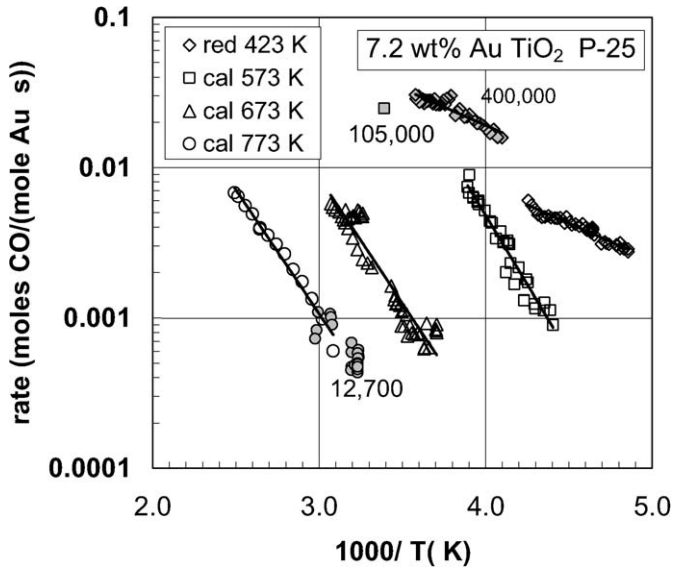

Fig. 4. Reaction rate of the 7.2 wt% Au/TiO_2 (P25) catalyst measured for various F/W ratios. Data is shown for four treatment temperatures and rates are measured at $F/W = 40{,}000$ mL CO/(g_{cat} h) (open symbols), or at the indicated F/W ratios (greyed symbols). Rate is expressed per total amount of Au in the catalyst (atomic rate).

ders of magnitude (see also Table 3) resulting from the thermal treatments. The increase in the coordination numbers (1NN) obtained by EXAFS suggests that the deactivation results from growth of the Au particles. It is of interest to relate the measured coordination numbers to mean Au particle sizes. This may be done using the EXAFS-derived 1NN coordination numbers, which can be related to the Au particle size using a geometric model for the Au particle structure. Previous studies of Au on three different polymorphs of TiO_2 by Z-contrast STEM have shown that the Au particles are raft-like, rather than spherical or a full cubo-octahedra, after reduction and calcination at low temperatures [19]. Therefore, a model was assumed in which the particles grow as a hemispherical cubo-octahedra, truncated by a {111} basal plane [25]. This model approximates multilayered, raft-like morphology and gives good results for describing supported Pt clusters. The average particle size, d, obtained using this model is provided in the last column of Tables 1 and 2. Using this relationship, it is possible to plot the atomic rate as a function of particle size (instead of 1NN coordination number); Fig. 5 plots all of the atomic rates from Table 3 in this manner. Because there are variations in the measured activation energies and errors due to extrapolation, this process was done for two different temperatures, chosen as 273 and 298 K. Fig. 5 shows that the rates correlate with particle size, and because the

Table 3
Catalytic reaction rates for two temperatures for 1% CO in air

Treatment T (K)	W_{cat} (Mg)	F/W ($\times 10^{-3}$) (mL/(g_{cat} h))	E_a (kJ/mol)	Atomic rate (CO/(total Au s))	TOF (s^{-1})	Atomic rate (CO/(total Au s))	TOF (s^{-1})
	7.2 wt% Au–TiO_2 (P25)			Temperature = 298 K		Temperature = 273 K	
423	6.3	400	9.4	3.9E−02	7.9E−02	2.8E−02	5.6E−02
423	43.1	41	9.4	1.6E−02	3.1E−02	1.1E−02	2.2E−02
573	6.3	400	30.7	4.8E−03[b]	9.6E−03[b]	1.5E−03[b]	3.0E−03[b]
573	20.7	101	at T[a]	2.5E−02	4.9E−02	1.6E−02	3.2E−02
573	47	41	29.1	5.2E−02	1.0E−01	2.0E−02	4.0E−02
573	43.1	41	35.2	7.3E−02	1.5E−01	N/A	N/A
623	20.7	101	at T[a]	4.5E−03	1.3E−02	N/A	N/A
673	20.7	41	at T[a]	1.3E−03	5.6E−03	2.5E−04	1.1E−03
673	47	41	at T[a]	1.1E−03	4.8E−03	6.0E−04	2.7E−03
673	43.1	41	31.9	2.2E−03	9.8E−03	N/A	N/A
723	20.7	41	23.4	8.8E−04	5.7E−03	3.5E−04	2.3E−03
723	47	41	28.5	6.6E−04	4.3E−03	4.2E−04	2.7E−03
773	20.7	41	22.1	3.5E−04	3.6E−03	1.4E−04	1.4E−03
773	47	13	24.2	3.5E−04	3.5E−03	1.4E−04	1.4E−03
773	47	41	24.2	3.2E−04	3.3E−03	1.1E−04	1.1E−03
773	43.1	41	31.5	2.8E−04	2.8E−03	N/A	N/A
	4.5 wt% Au–TiO_2 (P25)			Temperature = 298 K		Temperature = 273 K	
423	49	40	22.5	8.8E−03[b]	1.6E−02[b]	3.1E−03[b]	5.6E−03[b]
423	49	40	9.4	2.4E−02	4.2E−02	1.7E−02	3.0E−02
573	49	40	21.0	2.5E−02	5.2E−02	1.1E−02	2.4E−02
573	49	40	21.6	2.6E−02	5.5E−02	2.4E−02	5.1E−02
623	49	40	27.7	2.4E−02	6.3E−02	8.8E−03	2.3E−02
673	49	40	27.7	2.4E−03	1.2E−02	8.5E−04	4.3E−03
673	49	40	30.9	6.4E−03	3.2E−02	2.1E−03	1.0E−02
723	49	40	32.5	2.4E−03	1.4E−02	7.0E−04	4.2E−03
773	49	40	19.3	5.4E−04	7.1E−03	2.6E−04	3.4E−03
773	49	40	28.2	8.3E−04	1.1E−02	2.9E−04	3.8E−03

[a] Values measured at target temperature only.
[b] These values circled in Fig. 5 and identified as anomalously low.

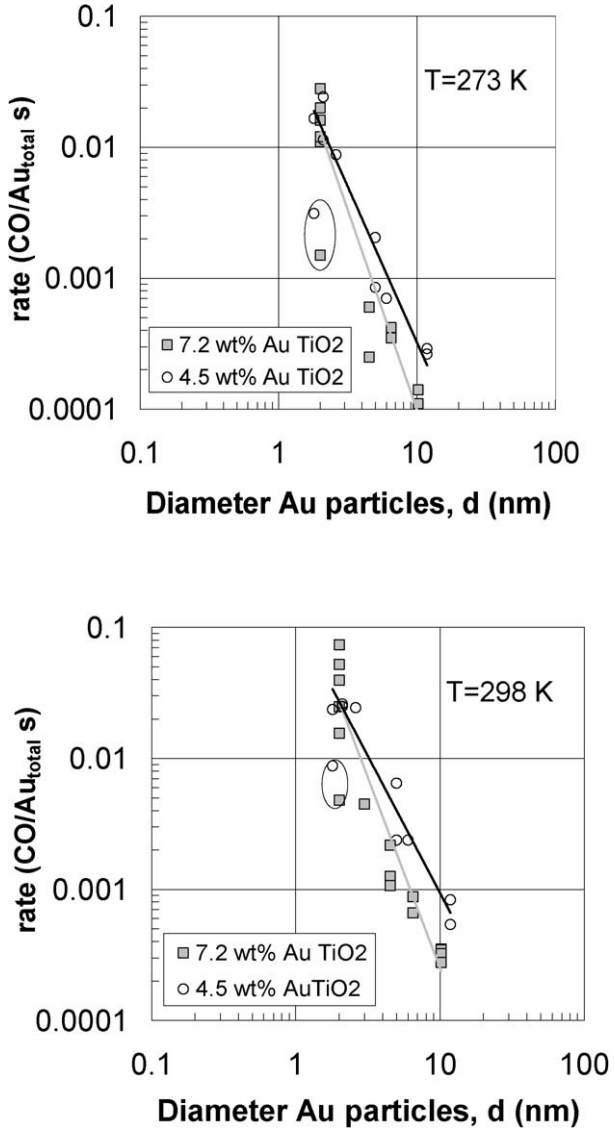

Fig. 5. Summary of the activity at 298 K (bottom) and at 273 K (top) for the two samples following all calcination steps leading to increasing particle size. Rate is expressed per total amount of Au (atomic rate). Best power law fits to the data (excluding the two encircled points) are shown for each catalyst.

data are presented as log–log plots, the correlation can be easily assessed by power law dependence. The power law dependence for each catalyst was extracted from a linear regression of all of the logarithmic data. The atomic rates at 298 K varied as $d^{-2.7\pm0.3}$ for the 7.2 wt% catalyst and $d^{-1.9\pm0.2}$ for the 4.5 wt% catalyst. Comparable results were obtained at 273 K, where the atomic rates varied only slightly faster as $d^{-2.8\pm0.3}$ and $d^{-2.1\pm0.3}$ for these two catalysts, respectively. Note that one data point for each catalyst (the circled values in Figs. 5a and b) seemed to be anomalously lower than expected for reasons that could not be determined. Ignoring these two points, the values of the exponents increased slightly to -2.9 ± 0.2 and -2.1 ± 0.2 at 298 K for the 7.2 wt% catalyst and -3.0 ± 0.3 and -2.4 ± 0.2 at 273 K for the 4.5 wt% catalyst.

Part of the activity decrease with particle size can be attributed to trivial loss of surface area. To account for this factor, the activity must be expressed on the basis of surface Au rather than total Au, that is, as a turnover frequency (TOF). The fraction of the total Au on the surface can be obtained from the surface-to-volume atomic ratio (i.e., the Au dispersion), and this can be used to compute the TOF. For a given spherical (or hemispherical) particle [26],

$$\text{dispersion} = \pi d^2 \rho_s / (\pi d^3/6)\rho_b,$$

where ρ_b is the bulk atomic density and ρ_s is the surface atomic areal density. Assuming that the Au particles are crystalline with bulk Au lattice constant $a_0 = 0.408$ nm, ρ_b is given by $4/a_0$ [3], and the ρ_s for the low-index surfaces (111), (100), and (110) are given by is $(4/\sqrt{3})a_0^{-2}$, $2a_0^{-2}$, and $\sqrt{2}a_0^{-2}$, respectively. Using these values in the above equation, the dispersion is given by

$$\text{dispersion} = \alpha/d \quad (\text{for } d > \alpha),$$

where the constant of proportionality α is 1.41, 1.22, or 0.865 for particles faceted primarily on the (111), (100), or (110) surface. If the small particles are rough and low coordinated, then it is reasonable to assume that α is near unity, whereas for well-ordered icosahedra, α can be up to 40% larger. Dividing the atomic rate by the dispersion (i.e., multiplying by d/α) yields the rate per surface Au (TOF). Therefore, in the range of 298–300 K, because the atomic rates vary approximately as $d^{-2.8}$ and $d^{-2.0}$ for the 7.2 and 4.5 wt% catalysts, the TOF must vary as $d^{-1.8}$ and $d^{-1.0}$, respectively. For a catalyst that is not size- or structure-dependent, the TOF is expected to be independent of d. Obviously, both catalysts confirm previous results indicating that the intrinsic activity of Au for CO oxidation is dependent on Au particle size.

Inspection of the data shown in Fig. 5 (and given in Table 3) shows a systematic variation between the two catalysts. The atomic rates were generally higher for the 4.5 wt% loading catalyst than for the 7.2 wt% catalysts. Because these are compared in Fig. 5 for a given particle size, the TOF also must be higher for the lower-loaded catalyst. Therefore, this trend could not be due to the possibility that the higher weight loading simply leads to a larger mean particle size and hence lower activity. Besides the different activities, there was also a statistically significant difference in the values of the exponent in the power law dependence for the two catalysts. The reasons for these differences are not known. One possibility is the effect of Cl^- poisoning; however, the possibility that the higher-weight-loaded catalyst may exhibit greater poisoning by Cl^- is not sustained by the analysis results, which instead indicate comparable overall Cl^- impurity levels in the two catalysts, and thus a lower Cl^-/Au atomic ratio at the less active, higher Au-loaded sample. One difference between the catalysts is that for a given mean particle size and fixed support surface area, the number density of Au particles must be smaller for the more active, lower-loaded sample. If the Au particles interact in some way (e.g., mutual heating, reaction at particle contacts, spillover), then the interaction must lead to inhibition of the reaction, because the more densely loaded support has the lower TOF. Note that given the weight loadings and surface areas of the TiO_2 supports, the Au particles can cover no more than 30% of the

TiO_2 surface, even for monolayer-dispersed Au [19]. This effect of total Au loading is a subject for further study.

There is a large spread in the data for the catalyst with the smallest particle size. Samples with the smallest sizes were typically measured at lower temperatures, requiring extrapolation to the comparison temperature, 298 K. In addition, the samples treated at 423 K tended to exhibit lower activation energies, around 9 kJ/mol, compared with 25–35 kJ/mol for those treated at 573 K and above. Such a low activation barrier may indicate that a different reaction mechanism is controlling the reaction rate. Low activation barriers frequently signal mass transfer limitations [26]; however, this was not the case here, because mild calcination increases the activation energy, and such calcination is not expected to affect mass transfer properties because it does not disturb or alter the bed geometry or significantly alter the morphology of the support particles. In addition, variation in activation energy complicates estimation of rates by extrapolation. Variation in reaction mechanism with temperature has been proposed previously to explain variations in the apparent E_a observed in various reaction temperature ranges [30]. If the reaction mechanism changed due to different reaction intermediates, or different types of sites, then it is certainly likely that the mechanism for size dependence would be altered. Competing reaction mechanisms could lead to variations that would appear as a spread in the reaction rates. A treatment temperature of 423 K is only partly effective in removing water from the sample, so after this treatment, the samples may have variable amounts of surface hydroxyls or more chemisorbed water than those treated at 573 K or higher. Water has been demonstrated to have an effect on the activity for CO oxidation [5,6], as described in the Bond–Thompson mechanism [31].

Perhaps the first description of the size dependence in Au catalysts was provided by Haruta et al. [1]. They suggested that the activity is limited by the availability of sites for oxygen adsorption, and that these sites are located at the interfacial perimeter around the Au metal particles. They pointed out that this could lead to a sharp size dependence, which should vary with varying d^{-2}. To clarify, the ratio of Au atoms located at the interfacial perimeter of a supported hemispherical cap with diameter d to the total number of Au atoms in the cap volume would be expected to vary as d^{-2}, but the ratio of these sites to the number of Au atoms on the surface of the cap should vary as d^{-1}. Therefore, the atomic rate should vary as d^{-2}, whereas the TOF should vary as d^{-1}. This dependence agrees well with the results for the 4.5 wt% catalyst but is slower than that observed for the higher-loaded catalysts. The actual dependence for peripheral sites may be expected to depend strongly on the aspect ratio and shape of the Au particles and the nature of the contact between the particles and the support.

Factors that are expected to relate to the size effect in Au particles have been considered theoretically [16,17]. Using density functional computations, Mavrikakis et al. [17] demonstrated that the adsorption of CO, O_2, and O on a Au surface is stabilized at steps. They argued that the ability of the Au surface to interact with the adsorbates is a function of the reaction barrier. They therefore concluded that the increasing density of steps expected with decreasing Au cluster size provides an explanation for the size-dependent activity. Based on a Wulff-like construction and experimentally observed aspect ratios of Au particles on TiO_2, they presented a model for the fraction of step sites per *total* Au atoms as a function of Au cluster size. In the range of sizes of about 1.5–10 nm, this step density is approximated by a $d^{-1.6}$ dependence. Based on this model, the atomic rate should vary as $d^{-1.6}$, and the TOF should vary as $d^{-0.6}$. Both of the present catalysts appear to vary more strongly, suggesting that the most active sites are lower coordinated than step sites.

In a more recent paper, Lopez et al. [16] continued the examination of size dependence using many of the earlier approaches and comparing existing published activity data for Au catalysts on various supports. They more generally concluded that lower coordination sites provide more stable adsorption sites and thus are more reactive. They accumulated literature data for atomic rates (mol CO/(total mol Au s)) suggesting d^{-3} dependence for the atomic rate. They also suggested that such dependence can apply if only corner-type sites on Au particles contribute to the activity. It can be seen that this dependence adequately describes the data for the 7.2 wt% catalyst in the present work. Effects of strain, charge transfer to the Au particle from the support, state of the Au particle (metallic to insulating), and intrinsic quantum size have less effect than the Au atom coordination. This slower variation in the observed rate, at least for the lower-weight-loaded Au, suggests that the dimensionality of the sites is less constrained than for corner sites only.

Size dependence is certainly not limited to Au particles. It is well known in catalysis and occurs for many reactions and many different types of metals [14,32]. Before the earliest references to size dependence in Au catalysts, Che and Bennett reviewed experimental data that exhibit size dependence for numerous different reactions [14]. Depending on the reaction, the experimentally measured TOF may increase or decrease with increasing particle size or may exhibit a maximum at an optimal size, generally in the range of 1–10 nm. In many cases, the variation in TOF may be as much as two orders of magnitude. However, CO oxidation is not generally a size-sensitive reaction. The characteristic that makes Au rather unusual is its large variation in TOF for this reaction with very low activity for bulk Au. In comparison, Pt, Pd, and Ir exhibit much less structure sensitivity [14]. Using well-characterized Pt/SiO_2 catalysts, Herskowitz found that TOF increased with increasing particle size (i.e., opposite to Au) but by at most about a factor of 2–3 in the range of 1.4–3 nm [33,34]. Bamwenda et al. [2] reported increases by about a factor of 3 in this range, whereas other results show little or no sensitivity [33,35,36] in conditions in which the CO/O_2 ratio is not too low.

The present results provide no strong evidence that a maximum activity occurs with decreasing activity as the particles shrink to atomic clusters. By the current preparation methods, particles smaller than about 2 nm (1NN around 8) were obtained only with the samples that had not been calcined at above 425 K. However, the activity likely does decrease for sufficiently small Au clusters. This prediction is based on general size-dependent behavior of metal clusters and on specific

results for Au. Che and Bennett [14] concluded from examination of many "supported small metal and naked metal clusters" that "the TOF tends to zero as the number of atoms per particle tends to unity." In addition, measurements of CO_2 temperature-programmed reaction from supported Au clusters suggest that Au clusters with fewer than about eight atoms are inactive [37]. In the gap between few-atom clusters and 2-nm particles, the electronic properties are expected to vary considerably, but should achieve bulk-like characteristics when the particles achieve dispersions of less than about 50%, that is, larger than about 2 nm. XPS provides evidence that particles larger than this range become bulk-like [14]. Therefore, the decrease in activity above 2 nm observed in the present work must have a different origin than variation of the overall particle electronic properties. From the d dependence, it seems likely that the variation is due to a particular type of low-coordinated site. The activity of low-coordinated sites (kinks) or special multicoordinated sites (B5 sites or Au-support periphery sites), which support the d^{-2} dependence in TOF, are likely models. Although the overall electronic properties of these >2-nm Au particles may be bulk-like, the active low-coordinated (or periphery) sites undoubtedly have special local electronic structures that are manifestations of their geometry and are responsible for the high activity.

These results suggest that the key to achieving high activity is to synthesize and stabilize Au particles with a preponderance of Au atoms in as-yet unidentified optimal coordination site. Currently, the only way to approximate this in practical catalysts is to stabilize particles of optimal size, although the fraction of any given type of low-coordinated sites may depend more on the geometry of the particle than on the size. Evidence for this is provided by results of Chen and Goodman, who achieved very high turnovers from a well-defined Au overlayer with uniform structure [13]. Interaction of the support with a Au particle is expected to have an effect on its resulting shape and contact area between the Au and the support. Therefore, tailoring support properties may permit optimization of the Au particle geometry and hence its activity. Such structural considerations may play a role in observed support-dependent variation in Au activity.

5. Conclusion

In this work, the size dependence of CO oxidation activity was measured for two Au catalysts that were systematically annealed to vary the Au particle size. Through this approach, the effects of other factors affecting the activity (e.g., support type, Au loading, impurity concentration) were minimized. The TOF decreased with particle size approximately as $d^{-1.8}$ for the 7.2 wt% catalysts and $d^{-1.0}$ for the 4.5 wt% catalyst, for mean particle size in the range of 2–10 nm. The discrepancy between the two catalysts emphasizes the sensitivity of the Au catalysts to other factors that may be difficult to control. It is concluded that the origin of the dependence in this size range was due not to size-dependent variation in overall electronic properties of the Au nanoparticles, but rather to variation in the relative numbers of low-coordinated or periphery sites with special catalytic properties. It appears that the dependence was steeper than expected for step sites, but the most active sites may be due to sites with still-lower coordination (e.g., kinks) or to sites at the support–Au particle interface.

Acknowledgments

This research was sponsored by the Division of Chemical Sciences, Geosciences, and Biosciences, Office of Basic Energy Sciences, US Department of Energy, under contract DE-AC05-00OR22725 with Oak Ridge National Laboratory, managed and operated by UT-Battelle, LLC. W. Yan is sponsored by an appointment to the Oak Ridge National Laboratory Postdoctoral Research Associates Program administered jointly by the Oak Ridge Institute for Science and Education and Oak Ridge National Laboratory. A portion of this work was performed at the National Synchrotron Light Source at Brookhaven National Laboratory, which is supported by Basic Energy Sciences, US Department of Energy under contract DE-AC02-98CH10886.

References

[1] M. Haruta, S. Tsubota, T. Kobayashi, H. Kageyama, M.J. Genet, B. Delmon, J. Catal. 144 (1993) 175–192.
[2] G.R. Bamwenda, S. Tsubota, T. Nakamura, M. Haruta, Catal. Lett. 44 (1997) 83–87.
[3] M.M. Schubert, S. Hackenberg, A.C. van Veen, M. Muhler, V. Plzak, R.J. Behm, J. Catal. 197 (2001) 113–122.
[4] S.H. Overbury, L. Ortiz-Soto, H.G. Zhu, B. Lee, M.D. Amiridis, S. Dai, Catal. Lett. 95 (2004) 99–106.
[5] M. Date, M. Haruta, J. Catal. 201 (2001) 221–224.
[6] C.K. Costello, J.H. Yang, H.Y. Law, Y. Wang, J.N. Lin, L.D. Marks, M.C. Kung, H.H. Kung, Appl. Catal. A Gen. 243 (2003) 15–24.
[7] H. Oh, C. Costello, C. Cheung, H. Kung, M. Kung, Proc. Stud. Surf. Sci. Catal. 139 (2001) 375–381.
[8] V. Schwartz, D.R. Mullins, W.F. Yan, B. Chen, S. Dai, S.H. Overbury, J. Phys. Chem. B 108 (2004) 15782–15790.
[9] M. Okumura, S. Nakamura, S. Tsubota, T. Nakamura, M. Azuma, M. Haruta, Catal. Lett. 51 (1998) 53.
[10] M. Okumura, S. Nakamura, S. Tsubota, T. Nakamura, M. Haruta, Prep. Catal. VII 118 (1998) 277–284.
[11] R. Zanella, S. Giorgio, C.R. Henry, C. Louis, J. Phys. Chem. B 106 (2002) 7634–7642.
[12] M. Valden, X. Lai, D.W. Goodman, Science 281 (1998) 1647–1650.
[13] M.S. Chen, D.W. Goodman, Science 306 (2004) 252.
[14] M. Che, C.O. Bennett, Adv. Catal. 36 (1989) 55.
[15] R. van Hardeveld, F. Hartog, Adv. Catal. 22 (1972) 75.
[16] N. Lopez, T.V.W. Janssens, B.S. Clausen, Y. Xu, M. Mavrikakis, T. Bligaard, J.K. Norskov, J. Catal. 223 (2004) 232–235.
[17] M. Mavrikakis, P. Stoltze, J.K. Norskov, Catal. Lett. 64 (2000) 101–106.
[18] H. Hakkinen, W. Abbet, A. Sanchez, U. Heiz, U. Landman, Angew. Chem.-Int. Ed. 42 (2003) 1297–1300.
[19] W.F. Yan, B. Chen, S.M. Mahurin, V. Schwartz, D.R. Mullins, A.R. Lupini, S.J. Pennycook, S. Dai, S.H. Overbury, J. Phys. Chem. B 109 (2005) 10676–10685.
[20] M. Vaarkamp, J.C. Linders, D.C. Koningsberger, Physica B 209 (1995) 159.
[21] J.W. Cook, D.E. Sayers, Solid State Ionics 16 (1985) 23.
[22] A.L. Ankudinov, J.J. Rehr, Phys. Rev. B 56 (1997) 1712.
[23] J.H. Yang, J.D. Henao, C. Costello, M.C. Kung, H.H. Kung, J.T. Miller, A.J. Kropf, J.G. Kim, J.R. Regalbuto, M.T. Bore, H.N. Pham, A.K. Datye, J.D. Laeger, K. Kharas, Appl. Catal. A Gen. 291 (2005) 73–84.
[24] H.G. Fritsche, T. Buttner, Z. Phys. Chem.-Int. J. Res. Phys. Chem. Chem. Phys. 209 (1999) 93–101.

[25] A.I. Frenkel, C.W. Hills, R.G. Nuzzo, J. Phys. Chem. B 105 (2001) 12689–12703.
[26] R.J. Farrauto, C.H. Bartholomew, Fundamentals of Industrial Catalytic Processes, Blackie Academic and Professional, New York, 1997.
[27] M. Haruta, Catal. Today 36 (1997) 153–166.
[28] Y. Yuan, K. Asakura, H. Wan, K. Tsai, Y. Iwasawa, Catal. Lett. 42 (1996) 15.
[29] S.D. Lin, M. Bollinger, M.A. Vannice, Catal. Lett. 17 (1993) 245.
[30] M. Haruta, CATTECH 6 (2002) 102–115.
[31] G.C. Bond, D.T. Thompson, Gold Bulletin 33 (2000) 41–51.
[32] G.C. Bond, Surf. Sci. 156 (1985) 966–981.
[33] N.W. Cant, J. Catal. 74 (1981) 411–412.
[34] M. Herskowitz, R. Holliday, M.B. Cutlip, C.N. Kenney, J. Catal. 74 (1982) 408.
[35] N.W. Cant, J. Catal. 62 (1980) 173.
[36] E. McCarthy, J. Zahradnik, G.C. Kuczynski, J.J. Carberry, J. Catal. 39 (1975) 29.
[37] A. Sanchez, S. Abbet, U. Heiz, W.D. Schneider, H. Hakkinen, R.N. Barnett, U. Landman, J. Phys. Chem. A 103 (1999) 9573–9578.